AIMS Mathematics, 10(9): 21533–21548.
DOI: 10.3934/math.2025957
Received: 02 June 2025
Revised: 24 July 2025
Accepted: 04 August 2025
Published: 17 September 2025

https://www.aimspress.com/journal/Math

Research article

Computational study of soliton behavior in the simplified modified form of the Camassa-Holm equation

Hamida Parvin[1], Md. Nur Alam[1,2,*], Md. Farhad Hossain[1], Mohammad Hassan[3] and Md. Jakir Hossen[4,*]

[1] Department of Mathematics, Pabna University of Science and Technology, Pabna-6600, Bangladesh
[2] Department of Mathematics, Saveetha School of Engineering, Saveetha Institute of Medical and Technical Sciences, Chennai 602105, Tamil Nadu, India
[3] Department of Mathematics and Scientific Computing, Madan Mohan Malaviya University of Technology, Gorakhpur, U. P. 273 016, India
[4] Center for Advanced Analytics (CAA), COE for Artificial Intelligence, Faculty of Engineering & Technology (FET), Multimedia University, 75450 Melaka, Malaysia

* **Correspondence:** Email: nuralam.pstu23@gmail.com; nuralam23@pust.ac.bd; jakir.hossen@mmu.edu.my.

Abstract: This study offers an in-depth exploration of traveling wave solutions to the simplified modified Camassa-Holm (SMCH) equation through the application of the modified S-expansion method. Utilizing a traveling wave transformation, the SMCH equation is converted into a nonlinear ordinary differential equation, from which a wide range of exact solutions is systematically obtained. The modified S-expansion method, implemented using the Maple software, proves to be a robust and efficient analytical tool, yielding a variety of soliton solutions such as kink, bright, and dark solitons. To capture the intricate behavior of these solutions, MATLAB is employed to produce detailed 2D, 3D, and contour visualizations that reveal their structural features and propagation dynamics. A comparative assessment with the modified simple equation method and the $\exp(-\phi(\eta))$-expansion method highlights the modified S-expansion method's superior accuracy, simplicity, and adaptability to solve nonlinear partial differential equations. Significantly, the method also extends to fractional-order equations, showcasing its broad applicability in nonlinear system analysis. Key solutions are graphically represented under constrained parameter values to emphasize the core propagation features. Overall, this work enhances the current analytical methods to solve both

classical and fractional-order nonlinear partial differential equations (PDEs) and offers a valuable foundation for future research into closed-form traveling wave solutions across various disciplines.

Keywords: the simplified modified Camassa-Holm equation; modified S-expansion method; soliton solutions; nonlinear differential equations
Mathematics Subject Classification: 33F05, 35C08, 35E05, 35Q51, 37J25, 37L50

1. Introduction

Many researchers [1–16] have investigated the family of equations that takes the following form:

$$P_t - P_{xxt} + (\alpha + 1)PP_x = \alpha P_x P_{xx} + PP_{xxx}. \tag{1.1}$$

Equation (1.1) reduces to the Camassa-Holm (CH) equation when $\alpha = 2$ and takes the following form:

$$P_t - P_{xxt} + 3PP_x = 2P_x P_{xx} + PP_{xxx}. \tag{1.2}$$

Equation (1.1) reduces to the Degasperis-Procesi (DP) equation when $\alpha = 3$ and takes the following form:

$$P_t - P_{xxt} + 4PP_x = 3P_x P_{xx} + PP_{xxx}. \tag{1.3}$$

Both the CH and DP equations exhibit bi-Hamiltonian structures and are linked to corresponding isospectral problems [1]. They are formally integrable through the scattering and inverse scattering techniques [1]. Interestingly, these equations admit peaked solitary wave solutions, commonly known as peakons. While Eqs (1.2) and (1.3) share some structural resemblances, they are inherently different. In particular, the isospectral problem for the DP equation is third-order, whereas it is second-order for the CH equation [1]. Using the method of asymptotic integrability, Degasperis and Procesi [2] established that Eq (1.1) is only integrable when $\alpha = 2$ or $\alpha = 3$. The CH equation (1.2), which corresponds to when $\alpha = 2$, models shallow water waves and was initially derived as an approximation to the incompressible Euler equations. It was subsequently shown to be completely integrable, which led to a Lax pair formulation [2]. Likewise, the DP Eq (1.3), linked to when $\alpha = 3$, models shallow-water phenomena and has been proven to be integrable. Additionally, researchers have shown that Eq (1.1) supports single-peakon solutions and multi-peakon structures [2]. This study aims to build upon and advance the current research on the DP and CH equations. In particular, Wazwaz [3] introduced modified forms of these equations, which are presented as the modified DP and modified CH equations as follows:

$$P_t - P_{xxt} + 4P^2P_x = 3P_x P_{xx} + PP_{xxx}, \tag{1.4}$$

and

$$P_t - P_{xxt} + 3P^2P_x = 2P_x P_{xx} + PP_{xxx}, \tag{1.5}$$

respectively. Wazwaz [4] introduced a unified model that combines features of both the CH and DP equations, referred to as the general modified DP–CH equation, given by the following:

$$P_t - P_{xxt} + (\alpha + 1)P^2P_x = \alpha P_xP_{xx} + PP_{xxx}, \tag{1.6}$$

where $\alpha = 2$ and $\alpha = 3$. It is evident that the nonlinear convection term PP_x present in Eqs (1.2) and (1.3) is modified to P^2P_x in Eqs (1.5) and (1.6). Wazwaz [4] simplified Eq (1.6) according to modified form of the CH equation by setting $\alpha = 2$, which led to the following:

$$p_t - p_{xxt} + 3p^2p_x - 2p_xp_{xx} - pp_{xxx} = 0. \tag{1.7}$$

The following integrable CH equation for water waves was developed by Camassa and Holm [5]:

$$P_t - P_{xxt} + 2\alpha P_x + kPP_x = 2P_xP_{xx} + PP_{xxx}, \tag{1.8}$$

which kept two terms that are typically neglected in the shallow water, small amplitude limit.

The following modified CH equation was studied by Tian and Song [6]:

$$P_t - P_{xxt} + 2\alpha P_x + kP^nP_x = 2P_xP_{xx} + PP_{xxx}, \tag{1.9}$$

which acquired fresh peaking solutions for lone waves. Furthermore, Boyd [7] found that the two additional terms on the right-hand side of (1.8) were minimal if the solitary wave slowly varied with $\varrho = x - ct$; the solutions gave the soliton the lowest order as follows:

$$P_t - P_{xxt} + 2\alpha P_x + k\mathrm{P}P_x = 0. \tag{1.10}$$

Wazwaz [8] examined a modified version of the CH equation, which was derived from the modified CH (MCH) equation and simplified in light of (1.10) as follows:

$$P_t - P_{xxt} + 2\alpha P_x + kP^nP_x = 0. \tag{1.11}$$

In this study, we only consider $n = 2$ of Eq (1.11):

$$p_t + 2\beta p_x - p_{xxt} + kp^2p_x = 0 \ , \beta \in \Re, \ k > 0, \tag{1.12}$$

where $p(x,t)$ is a function that specifies the height of the sea surface or the amplitude of waves, and x and t are coordinates of space and time. This equation has garnered significant attention from the research community due to its broad relevance in modeling a wide range of wave phenomena [9]. Its study is of interest not only to mathematicians and physicists but also to engineers and experts in fields such as fluid dynamics, nonlinear optics, and image processing [10]. In particular, the simplified modified form of the CH equation plays a crucial role in analyzing wave behavior, and its numerous applications remain an active area of exploration [11]. Ali et al. [12] obtained accurate traveling wave solutions to the SMCH equation, presenting wave structures characterized by hyperbolic, trigonometric, exponential, and rational function forms. Islam et al. [13] studied the exact solutions of the simplified modified Camassa-Holm (SMCH)equation, and emphasized its wide applicability across the fields of mathematics, physics, and engineering. In this paper, we use the modified equation form as a basis to explore the changes in the physical nature of the solutions, from peakon solutions illustrated in Eq (1.3) to bell-shaped solitary waves and soliton structures expressed as ratios of exponential functions [14]. To conduct this investigation, we utilize the modified S-expansion method [15]. The modified S-expansion method is a powerful and efficient tool to solve nonlinear partial differential equations (PDEs), thereby offering a broad solution space, enhanced flexibility, reduced computational complexity, and adaptability to various physical models

and boundary conditions across diverse scientific and engineering fields. Despite its strengths, the modified S-expansion method has limitations, including the difficulty with highly nonlinear terms, the reliance on specific assumptions and parameter choices, a limited generalizability, and the reduced effectiveness for numerical or high-dimensional problems, which makes it best suited for select classes of nonlinear PDEs. The main steps of this method are presented in the following sections.

2. Materials and methods

We consider the following:

$$P(W, \frac{\partial W}{\partial t}, \frac{\partial W}{\partial x}, \frac{\partial^2 W}{\partial^2 x}, \frac{\partial^2 W}{\partial t \partial x}, \frac{\partial^2 W}{\partial^2 t}, \cdots\cdots) = 0. \tag{2.1}$$

First, we use the travelling variable as follows:

$$W(\Omega) = W(x,t), \Omega = x - ct. \tag{2.2}$$

Placing Eq (2.2) into Eq (2.1), we obtain the following:

$$F(W, W', W'', \cdots\cdots) = 0. \tag{2.3}$$

Again, we consider the following ansatz equation:

$$\Theta(\xi) = E_0 + \sum_{i=1}^{M} [E_i \{N(\xi)\}^i + \frac{F_i}{\{N(\xi)\}^i}], \tag{2.4}$$

where $N(\xi)$ satisfies

$$N'(\xi) = \vartheta_0 + \vartheta_0 N(\xi) + \vartheta_0 N(\xi)^2; \tag{2.5}$$

the values of ϑ_L, where $0 \leq L \leq 2$, can be found in Table 1 [16]. The values of E_i and F_i will be determined at a later stage.

Table 1. Relationships between $(\vartheta_0, \vartheta_1, \vartheta_2)$ and the function $N(\xi)$.

$(\vartheta_0, \vartheta_1, \vartheta_2)$	$N(\xi)$
$(\vartheta_0 = 0.5, \vartheta_1 = 0.0, \vartheta_2 = 0.5)$	$N(\xi) = sec(\xi) + tan(\xi)$. $N(\xi) = csc(\xi) + cot(\xi)$. $N(\xi) = sec(\xi) - tan(\xi)$. $N(\xi) = csc(\xi) - cot(\xi)$.
$(\vartheta_0 = \pm 1.0, \vartheta_1 = 0.0, \vartheta_2 = \pm 1.0)$	$N(\xi) = tan(\xi)$. $N(\xi) = cot(\xi)$.
$(\vartheta_0 = 0.0, \vartheta_1 = 1.0, \vartheta_2 = -1.0)$	$N(\xi) = \frac{1}{2}(1 + tanh(\frac{1}{2}\xi))$.
$(\vartheta_0 = 1.0, \vartheta_1 = 0.0, \vartheta_2 = -1.0)$	$N(\xi) = tanh(\xi)$. $N(\xi) = coth(\xi)$.
$(\vartheta_0 = 0.5, \vartheta_1 = 0.0, \vartheta_2 = -0.5)$	$N(\xi) = tanh(\xi) \pm sech(\xi)$. $N(\xi) = coth(\xi) \pm csch(\xi)$.

2.1. Flowchart of the modified S-Expansion method

A flowchart is a graphical representation of a process, sequence, or workflow, and utilizes standard symbols and connecting lines to illustrate the progression of steps. It simplifies complex tasks or decisions into clear, manageable stages, typically arranged from top to bottom or left to right. Flowcharts are widely employed across various fields—such as business process mapping, software development, troubleshooting, and education—to enhance our understanding, analysis, and optimization of workflows. In this section, we present a flowchart that outlines the steps of the modified S-expansion method. This visual aid provides a clear and systematic overview of the procedure of applying the method to nonlinear PDEs.

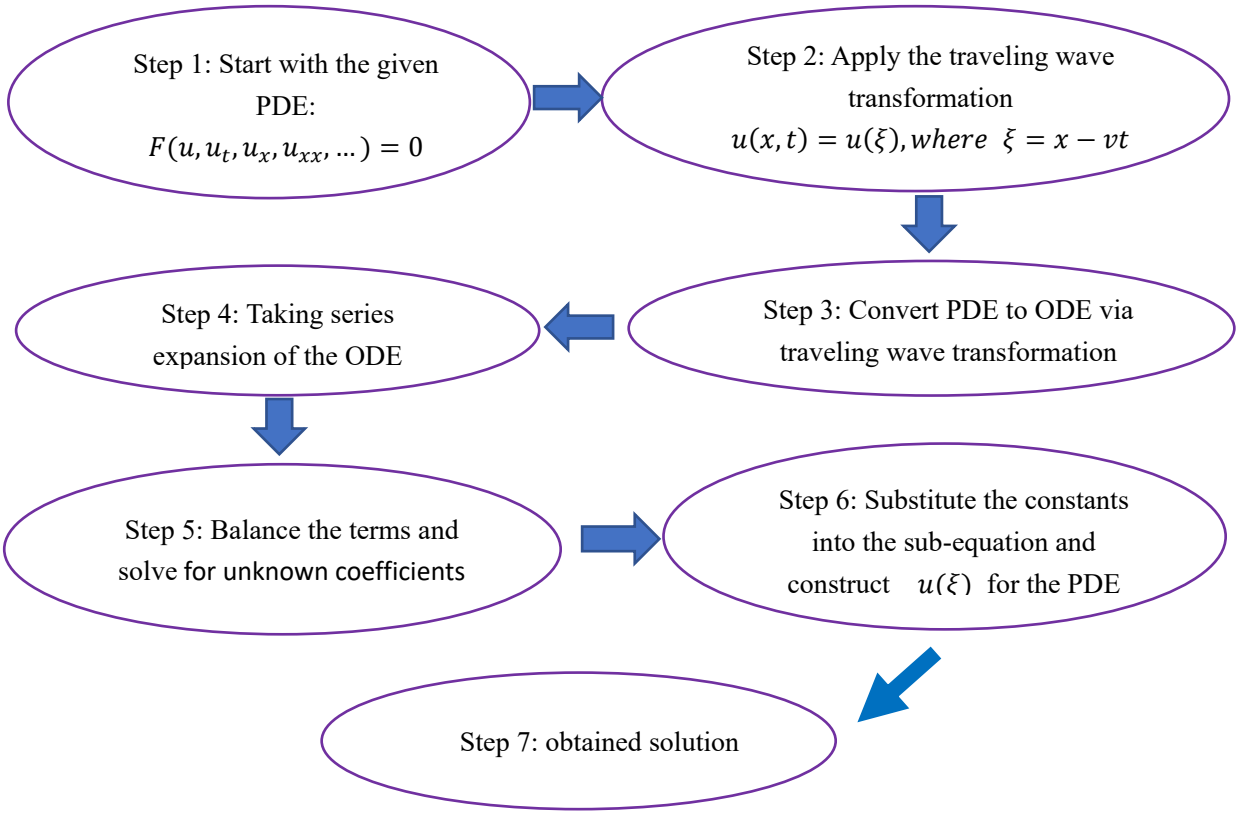

3. Solving the SMCH via the modified S-expansion method

Using the change of variables $p(x,t) = \Theta(\varrho)$ with $\varrho = x - ct$, Eq (1.12) is transformed into the following equation:

$$-c\Theta' + 2k\Theta' + c\Theta''' + \beta\Theta^2\Theta' = 0, \tag{3.1}$$

where the prime notation signifies the derivative with respect to the variable ϱ. Integrating Eq (3.1) concerning ϱ yields the following:

$$-c\Theta + 2k\Theta + \Theta''c + \frac{1}{3}\beta\Theta^3 + C = 0, \tag{3.2}$$

where C is a constant of integration.

Balancing the highest order linear and nonlinear terms appearing in Eq (3.2), we achieved $M = 1$. Therefore, we find the following:

$$\Theta = \lambda_0 + \lambda_1 N + \frac{q_1}{N}. \tag{3.3}$$

Then, by setting the coefficients of this polynomial equal to zero, a system of linear algebraic equations is formed, and the following set is obtained as its solution:

Set-I: $C = 0,\ c = -\frac{4k}{4\mu_0\mu_2-\mu_1^2-2},\ \lambda_0 = \mu_1\left(\pm\sqrt{\frac{6k}{4\beta\mu_0\mu_2-\beta\mu_1^2-2\beta}}\right),$

$$\lambda_1 = 0,\ q_1 = 2\mu_0\left(\pm\sqrt{\frac{6k}{4\beta\mu_0\mu_2-\beta\mu_1^2-2\beta}}\right).$$

Set-II: $C = 0,\ c = -\frac{4k}{4\mu_0\mu_2-\mu_1^2-2},\ \lambda_0 = \frac{6k\mu_1}{(4\mu_0\mu_2-\mu_1^2-2)\beta(\pm\sqrt{\frac{6k}{4\beta\mu_0\mu_2-\beta\mu_1^2-2\beta}})},$

$$\lambda_1 = 2\mu_2\left(\pm\sqrt{\frac{6k}{4\beta\mu_0\mu_2-\beta\mu_1^2-2\beta}}\right),\ \ q_1 = 0.$$

Set-III: $C = -\frac{96k^2\mu_1\mu_2\mu_0}{\beta(8\mu_0\mu_2+\mu_1^2+2)^2\left(\pm\sqrt{\left(\frac{-6k}{8\beta\mu_0\mu_2+\beta\mu_1^2+2\beta}\right)}\right)},\quad c = \frac{4k}{8\mu_0\mu_2+\mu_1^2+2}\ ,$

$$\lambda_0 = -\frac{6k\mu_1}{(8\mu_0\mu_2+\mu_1^2+2)\beta(\pm\sqrt{\left(\frac{-6k}{8\beta\mu_0\mu_2+\beta\mu_1^2+2\beta}\right)})},$$

$$\lambda_1 = 2\mu_2(\pm\sqrt{\left(\frac{-6k}{8\beta\mu_0\mu_2+\beta\mu_1^2+2\beta}\right)}),$$

$$q_1 = -\frac{12k\mu_0}{(8\mu_0\mu_2+\mu_1^2+2)\beta\left(\pm\left(\sqrt{\left(\frac{-6k}{8\beta\mu_0\mu_2+\beta\mu_1^2+2\beta}\right)}\right)\right)}.$$

Substituting the above values of Set-I in (3.3), then we achieve the following:

$$\Theta = \left[\mu_1\left(\pm\sqrt{\frac{6k}{4\beta\mu_0\mu_2-\beta\mu_1^2-2\beta}}\right) + 2\mu_0\left(\pm\sqrt{\frac{6k}{4\beta\mu_0\mu_2-\beta\mu_1^2-2\beta}}\right)\right] \times \frac{1}{N}. \tag{3.4}$$

If $\mu_0 = 0.5,\ \mu_1 = 0.0$, and $\mu_2 = 0.5$, then Eq (3.4) gives the following:

$$\Theta_1 = \pm\sqrt{\frac{6k}{-\beta}} \times \frac{1}{\sec(\xi)+\tan(\xi)}; \tag{3.5}$$

$$\Theta_2 = \pm\sqrt{\frac{6k}{-\beta}} \times \frac{1}{\csc(\xi)-\cot(\xi)}; \tag{3.6}$$

$$\Theta_3 = \pm\sqrt{\frac{6k}{-\beta}} \times \frac{1}{\sec(\xi)-\tan(\xi)}; \tag{3.7}$$

$$\Theta_4 = \pm\sqrt{\frac{6k}{-\beta}} \times \frac{1}{\csc(\xi)+\cot(\xi)}. \tag{3.8}$$

If $\mu_0 = \pm 1,\ \mu_1 = 0.0$, and $\mu_2 = \pm 1$, then Eq (3.4) gives the following:

$$\Theta_5 = 2\left[\pm\sqrt{\frac{6k}{\beta}}\right] \times \frac{1}{\tan(\xi)}; \tag{3.9}$$

$$\Theta_6 = 2\left[\pm\sqrt{\frac{6k}{\beta}}\right] \times \frac{1}{\cot(\xi)}. \tag{3.10}$$

If $\mu_0 = 0.0,\ \mu_1 = 1.0$, and $\mu_2 = -1.0$, then Eq (3.4) gives the following:

$$\Theta_7 = \pm\sqrt{\frac{6k}{-3\beta}} \times \frac{1}{\frac{1}{2}(1+tanh(\frac{1}{2}(\xi))}. \tag{3.11}$$

If $\mu_0 = 1.0,\ \mu_1 = 0.0$, and $\mu_2 = -1.0$, then Eq (3.4) gives the following:

$$\Theta_8 = 2\left[\pm\sqrt{\frac{k}{-\beta}}\right] \times \frac{1}{\tanh(\xi)}; \tag{3.12}$$

$$\Theta_9 = 2\left[\pm\sqrt{\frac{k}{-\beta}}\right] \times \frac{1}{\coth(\xi)}. \tag{3.13}$$

If $\mu_0 = 0.5,\ \mu_1 = 0.0$, and $\mu_2 = -0.5$, then Eq (3.4) gives the following:

$$\Theta_{10} = \pm\sqrt{\frac{2k}{-\beta}} \times \frac{1}{\tanh(\xi)\pm\mathrm{sech}(\xi)}; \tag{3.14}$$

$$\Theta_{11} = \pm\sqrt{\frac{2k}{-\beta}} \times \frac{1}{\coth(\xi)\pm\mathrm{csch}(\xi)}. \tag{3.15}$$

Substituting the above values of Set-II in Eq (3.3), then we achieve the following:

$$\Theta = \frac{6k\mu_1}{(4\mu_0\mu_2-\mu_1^2-2)\beta(\pm\sqrt{\frac{6k}{4\beta\mu_0\mu_2-\beta\mu_1^2-2\beta}})} + 2\mu_2\left(\pm\sqrt{\frac{6k}{4\beta\mu_0\mu_2-\beta\mu_1^2-2\beta}}\right) \times N. \tag{3.16}$$

If $\mu_0 = 0.5,\ \mu_1 = 0.0$, and $\mu_2 = 0.5$, then Eq (3.16) gives the following:

$$\Theta_{12} = \pm\sqrt{\frac{6k}{-\beta}} \times \sec(\xi) + \tan(\xi); \tag{3.17}$$

$$\Theta_{13} = \pm\sqrt{\frac{6k}{-\beta}} \times \csc(\xi) - \cot(\xi); \tag{3.18}$$

$$\Theta_{14} = \pm\sqrt{\frac{6k}{-\beta}} \times \sec(\xi) - \tan(\xi); \tag{3.19}$$

$$\Theta_{15} = \pm\sqrt{\frac{6k}{-\beta}} \times \csc(\xi) + \cot(\xi). \tag{3.20}$$

If $\mu_0 = \pm 1,\ \mu_1 = 0.0$, and $\mu_2 = \pm 1$, then Eq (3.16) gives the following:

$$\Theta_{16} = 2\left[\pm\sqrt{\frac{3k}{\beta}}\right] \times \tan(\xi)\,; \tag{3.21}$$

$$\Theta_{17} = 2\left[\pm\sqrt{\frac{2k}{\beta}}\right] \times \cot(\xi). \tag{3.22}$$

If $\mu_0 = 0.0,\ \mu_1 = 1.0$, and $\mu_2 = -1.0$, then Eq (3.16) gives the following:

$$\Theta_{18} = \pm\sqrt{\frac{6k}{-3\beta \pm \sqrt{\frac{2k}{-\beta}}}} - 2(\pm\sqrt{\frac{2k}{-\beta}} \times \frac{1}{2}(1 + tanh\left(\frac{1}{2}(\xi)\right). \tag{3.23}$$

If $\mu_0 = 1.0,\ \mu_1 = 0.0$, and $\mu_2 = -1.0$, then Eq (3.16) gives the following:

$$\Theta_{19} = -2\left[\pm\sqrt{\frac{k}{-\beta}}\right] \times \tanh(\xi)\,; \tag{3.24}$$

$$\Theta_{20} = -2\left[\pm\sqrt{\frac{k}{-\beta}}\right] \times \cot h(\xi). \tag{3.25}$$

If $\mu_0 = 0.5,\ \mu_1 = 0.0$, and $\mu_2 = -0.5$, then Eq (3.16) gives the following:

$$\Theta_{21} = -\left(\pm\sqrt{\frac{2k}{-\beta}}\right) \times (\tanh(\xi) \pm \operatorname{sech}(\xi)); \tag{3.26}$$

$$\Theta_{22} = -(\pm\sqrt{\frac{2k}{-\beta}}) \times (\coth(\xi) \pm \operatorname{csch}(\xi)). \tag{3.27}$$

Substituting the above values of Set-III in Eq (3.3), then we achieve the following:

$$\Theta = -\frac{6k\mu_1}{(8\mu_0\mu_2 + \mu_1^2 + 2)\beta\left(\pm\sqrt{\left(\frac{-6k}{8\beta\mu_0\mu_2 + \beta\mu_1^2 + 2\beta}\right)}\right) + 2\mu_2\left(\pm\sqrt{\left(\frac{-6k}{8\beta\mu_0\mu_2+\beta\mu_1^2+2\beta}\right)}\right) \times N - \frac{12k\mu_0}{(8\mu_0\mu_2+\mu_1^2+2)\beta\left(\pm\left(\sqrt{\left(\frac{-6k}{8\beta\mu_0\mu_2+\beta\mu_1^2+2\beta}\right)}\right)\right)} \times \frac{1}{N}}. \tag{3.28}$$

If $\mu_0 = 0.5,\ \mu_1 = 0.0$, and $\mu_2 = 0.5$, then Eq (3.28) gives the following:

$$\Theta_{23} = \pm\sqrt{\frac{-3k}{2\beta}} \times (\sec(\xi) + \tan(\xi)) - \left(\frac{6k}{4\beta \pm \sqrt{\frac{-3k}{2\beta}}}\right) \times \frac{1}{\sec(\xi)+\tan(\xi)}; \tag{3.29}$$

$$\Theta_{24} = \pm\sqrt{\frac{-3k}{2\beta}} \times (\csc(\xi) - \cot(\xi)) - \left(\frac{6k}{4\beta \pm \sqrt{\frac{-3k}{2\beta}}}\right) \times \frac{1}{\csc(\xi)-\cot(\xi)}; \tag{3.30}$$

$$\Theta_{25} = \pm\sqrt{\frac{-3k}{2\beta}} \times (\sec(\xi) - \tan(\xi)) - \left(\frac{6k}{4\beta \pm \sqrt{\frac{-3k}{2\beta}}}\right) \times \frac{1}{\sec(\xi) - \tan(\xi)}; \tag{3.31}$$

$$\Theta_{26} = \pm\sqrt{\frac{-3k}{2\beta}} \times (\csc(\xi) + \cot(\xi)) - \left(\frac{6k}{4\beta \pm \sqrt{\frac{-3k}{2\beta}}}\right) \times \frac{1}{\csc(\xi) + \cot(\xi)}. \tag{3.32}$$

If $\mu_0 = \pm 1,\ \mu_1 = 0.0$, and $\mu_2 = \pm 1$, then Eq (3.28) gives the following:

$$\Theta_{27} = 2\left[\pm\sqrt{\frac{-6k}{10\beta}}\right] \times (\tan(\xi)) - \left(\frac{12k}{10\beta(\pm\sqrt{\frac{-6k}{10\beta}})}\right) \times \frac{1}{\tan(\xi)}; \tag{3.33}$$

$$\Theta_{28} = 2\left[\pm\sqrt{\frac{-6k}{10\beta}}\right] \times (\cot(\xi)) - \left(\frac{12k}{10\beta(\pm\sqrt{\frac{-6k}{10\beta}})}\right) \times \frac{1}{\cot(\xi)}. \tag{3.34}$$

If $\mu_0 = 0.0,\ \mu_1 = 1.0$, and $\mu_2 = -1.0$, then Eq (3.28) gives the following:

$$\Theta_{29} = \pm\sqrt{\frac{6k}{3\beta(\pm\sqrt{\frac{-6k}{3\beta}})}} - 2(\pm\sqrt{\frac{-6k}{3\beta}}) \times \frac{1}{2}(1 + tanh\left(\frac{1}{2}(\xi)\right). \tag{3.35}$$

If $\mu_0 = 1.0,\ \mu_1 = 0.0$, and $\mu_2 = -1.0$, then Eq (3.28) gives the following:

$$\Theta_{30} = -2\left[\pm\sqrt{\frac{k}{\beta}}\right] \times \tanh(\xi) - \left(\frac{12k}{-6\beta(\pm\sqrt{\frac{k}{\beta}})}\right) \times \frac{1}{\tanh(\xi)}; \tag{3.36}$$

$$\Theta_{31} = -2\left[\pm\sqrt{\frac{k}{\beta}}\right] \times \coth(\xi) - \left(\frac{12k}{-6\beta(\pm\sqrt{\frac{k}{\beta}})}\right) \times \frac{1}{\coth(\xi)}. \tag{3.37}$$

4. Graphical representation

To make effective use of graphical representations, it is important to comprehend different types of graphs, such as 2D, 3D, contour, cyclic, and full graphs. Specifically, in the study of nonlinear partial differential equations, 2D, 3D, and contour plots play crucial roles in visualizing, analyzing, and understanding the behavior of soliton solutions. In this section, we focus on these three graph types, and emphasize their importance and relevance in soliton analysis. Additionally, we compare the outcomes obtained through our proposed methods with those from existing techniques applied to the same equations, thus highlighting the enhanced accuracy of our results.

The presented graphs visually depict the solutions of the SMCH equation for various parameter settings. Figure 1 represents the 2D for different fractional orders (α = 0.4, 0.5, 0.6, 0.8, and 0.9), 3D, and contour profiles for the multi-soliton shaped solution of Eq (3.7) for the different parameter values $k = 0.001,\ l = 0.002,\ c = 0.003,\ w_0 = 0.05,\ w_1 = 0.00,\ w_2 = 0.05,\ r_1 = 0.02,\ \beta = 4,\ \alpha = 0.7$, and $t = 10$. A multi-soliton-shaped solution describes the interaction of multiple solitary waves, each retaining its shape and speed after collision, which reflects the

integrability and stability of the underlying nonlinear system.

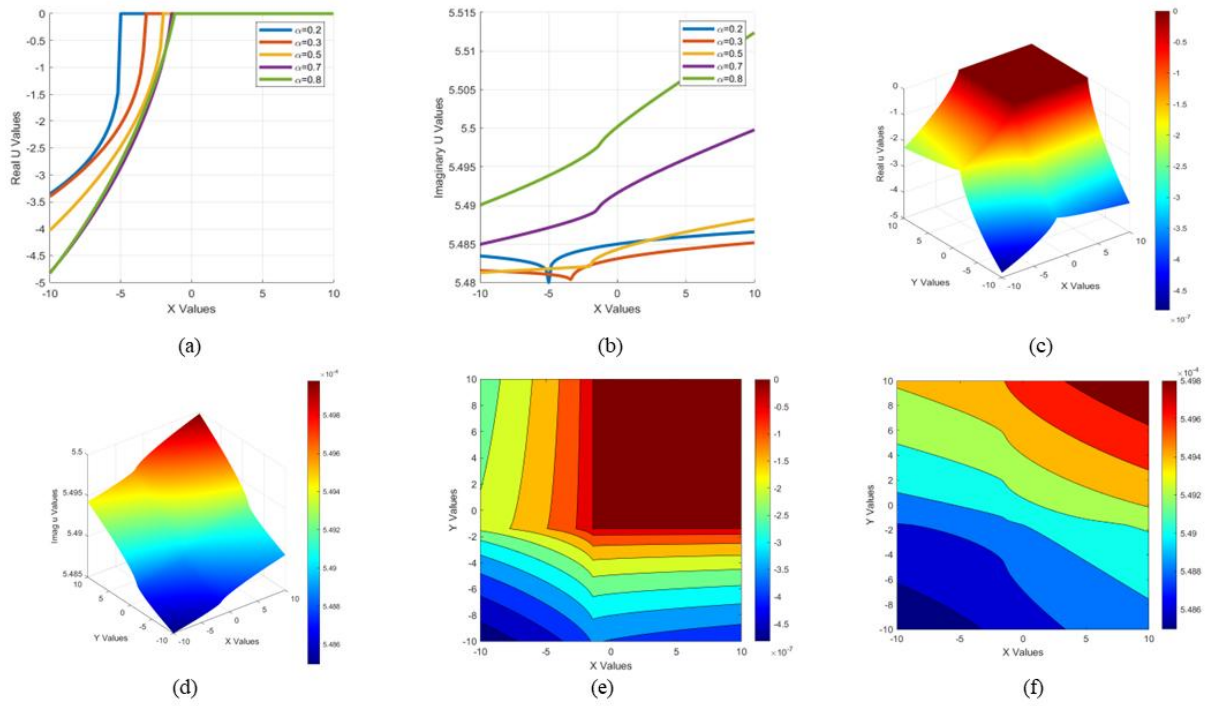

Figure 1. 2D, 3D, and contour profiles for the multi-soliton shaped solution of Eq (3.7) are obtained for certain values of $k = 0.001$, $l = 0.002$, $c = 0.003$, $w_0 = 0.05$, $w_1 = 0.00$, $w_2 = 0.05$, $r_1 = 0.02$, $\beta = 4$, and $t = 10$, thus showing its smooth transition and propagation over space and time.

Figure 2 represents 2D for different fractional orders (α = 0.4, 0.5, 0.6, 0.8, and 0.9), 3D, and contour profiles for the bright and dark soliton shaped solutions of Eq (3.9) for the different parameter values $k = 0.1$, $l = 0.2$, $c = 0.3$, $w_0 = 1.0$, $w_1 = 0.0$, $w_2 = -1.0$, $r_1 = 0.2$, $\beta = 2$, $\alpha = 0.5$, and $t = 10$. Bright solitons are localized, peak-shaped waves that arise in systems with focusing nonlinearity, thereby concentrating energy in a narrow region without a constant background, and are observed in various physical contexts such as optical fibers, water waves, plasmas, and Bose-Einstein condensates. A dark soliton-shaped solution features a localized drop in intensity or amplitude against a continuous wave background, typically arising in systems with defocusing nonlinearity, and is characterized by a phase shift across the soliton. Bright and dark solitons are unique wave solutions important for fluid dynamics because they exhibit stable, self-reinforcing structures capable of travelling great distances without changing the shape.

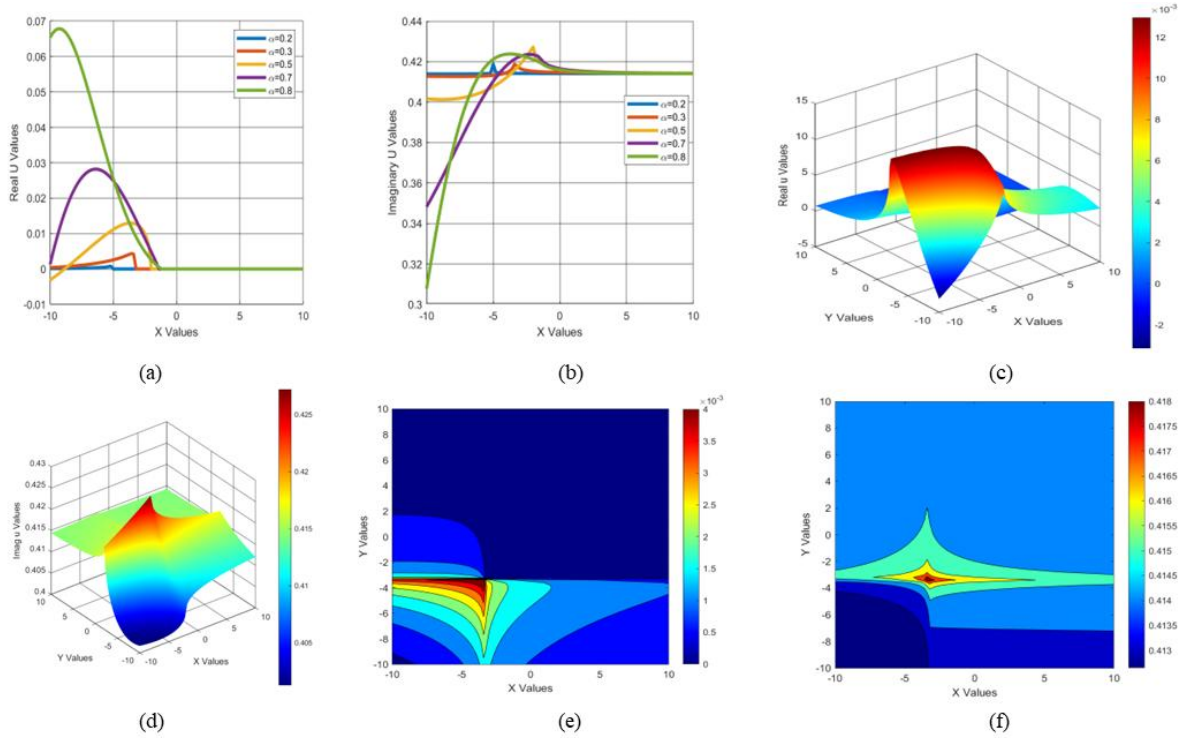

Figure 2. 2D, 3D, and contour profiles for the bright and dark soliton-shaped solutions of Eq (3.9) is obtained for certain values of $k = 0.1$, $l = 0.2$, $c = 0.3$, $w_0 = 1.0$, $w_1 = 0.0$, $w_2 = -1.0$, $r_1 = 0.2$, $\beta = 2$, $\alpha = .5$, and $t = 10$, thus showing its smooth transition and propagation over space and time.

Figure 3 represents the 2D for different fractional orders (α = 0.4, 0.5, 0.6, 0.8, and 0.9), 3D, and contour profiles for the bright multi-soliton-shaped solution of Eq (3.23) for the different parameter values $k = 0.1$, $l = 0.2$, $c = 0.3$, $w_0 = 0.0$, $w_1 = 1.0$, $w_2 = -1.0$, $r_1 = 0.2$, $\beta = 2$, $\alpha = 0.7$, and $t = 10$. A bright multi-soliton-shaped solution consists of multiple localized wave peaks that maintain their shape, speed, and amplitude during interactions, which typically occur in systems with focusing nonlinearity and demonstrate the coherence and stability of bright soliton dynamics.

Figure 4 represents the 2D for different fractional orders (α = 0.4, 0.5, 0.6, 0.8, and 0.9), 3D, and contour profiles for the plane wave soliton solution of Eq (3.26) for the different parameter values $k = 0.1$, $l = 0.2$, $c = 0.3$, $w_0 = 0.5$, $w_1 = 0.0$, $w_2 = -0.5$, $r_1 = 0.2$, $\beta = 2$, $\alpha = 0.5$, and $t = 10$. A plane wave soliton solution is characterized by a uniform amplitude and phase, non-decaying background, and evenly distributed energy, thus serving as a foundational structure to analyze soliton formation, modulation, and stability in nonlinear systems.

Figure 5 represents the 2D for different fractional orders (α = 0.4, 0.5, 0.6, 0.8, and 0.9), 3D, and contour profiles for the dark soliton solution of Eq (3.36) for the different parameter values $= 0.1$, $l = 0.2$, $c = 0.3$, $w_0 = 0.5$, $w_1 = 0.0, w_2 = 0.5$, $r_1 = 0.2$, $\beta = 2$, $\alpha = 0.8$, and $t = 10$.

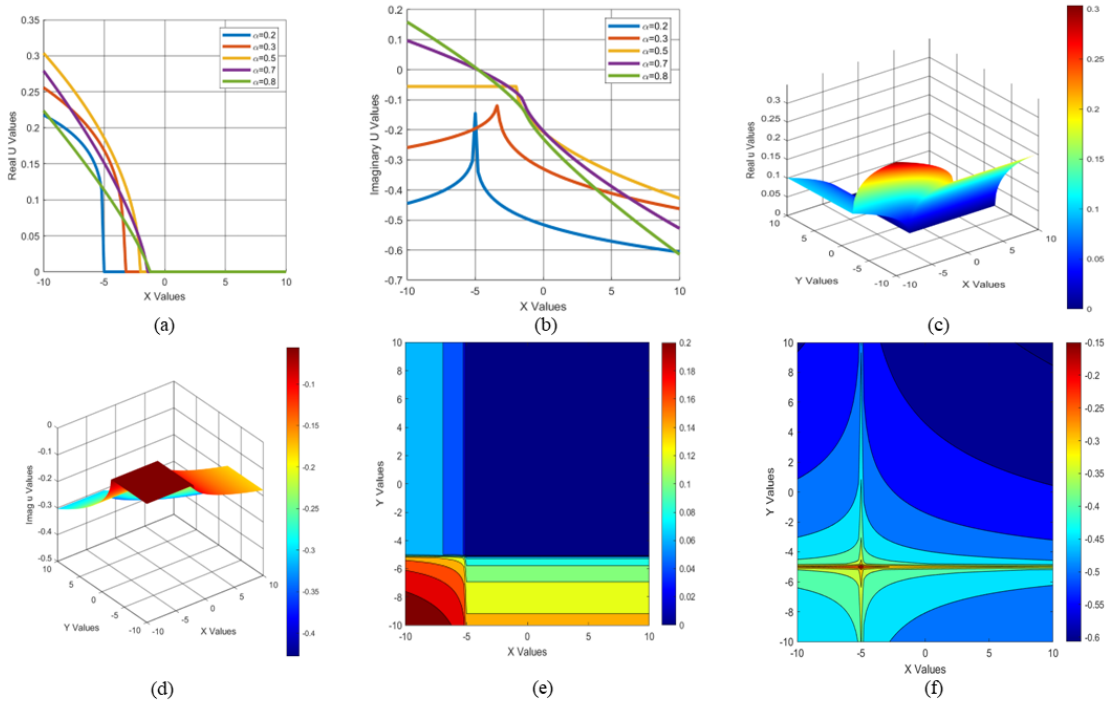

Figure 3. 2D, 3D, and contour profiles for the bright multi-soliton-shaped solution of Eq (3.23) is obtained for certain values of $k = 0.1$, $l = 0.2$, $c = 0.3$, $w_0 = 0.0$, $w_1 = 1.0$, $w_2 = -1.0$, $r_1 = 0.2$, $\beta = 2$, $\alpha = 0.7$, and $t = 10$, thus showing its smooth transition and propagation over space and time.

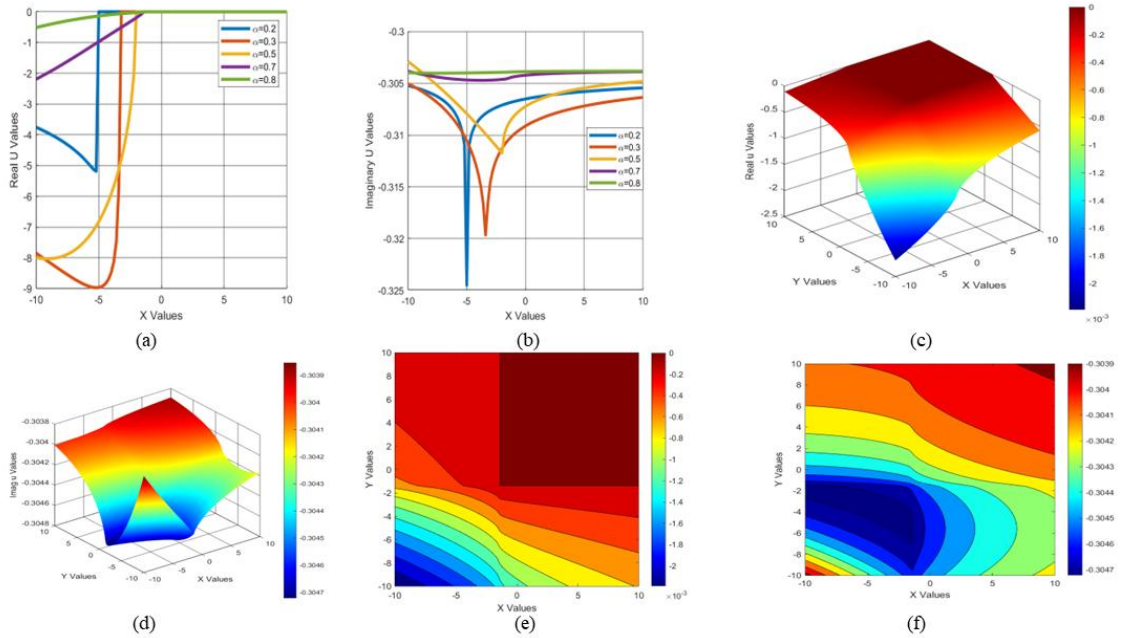

Figure 4. 2D, 3D, and contour profiles for the plane wave soliton solution of Eq (3.26) is obtained for certain values of $k = 0.1$, $l = 0.2$, $c = 0.3$, $w_0 = 0.5$, $w_1 = 0.0$, $w_2 = -0.5$, $r_1 = 0.2$, $\beta = 2$, $\alpha = 0.5$, and $t = 10$, thus showing its smooth transition and propagation over space and time.

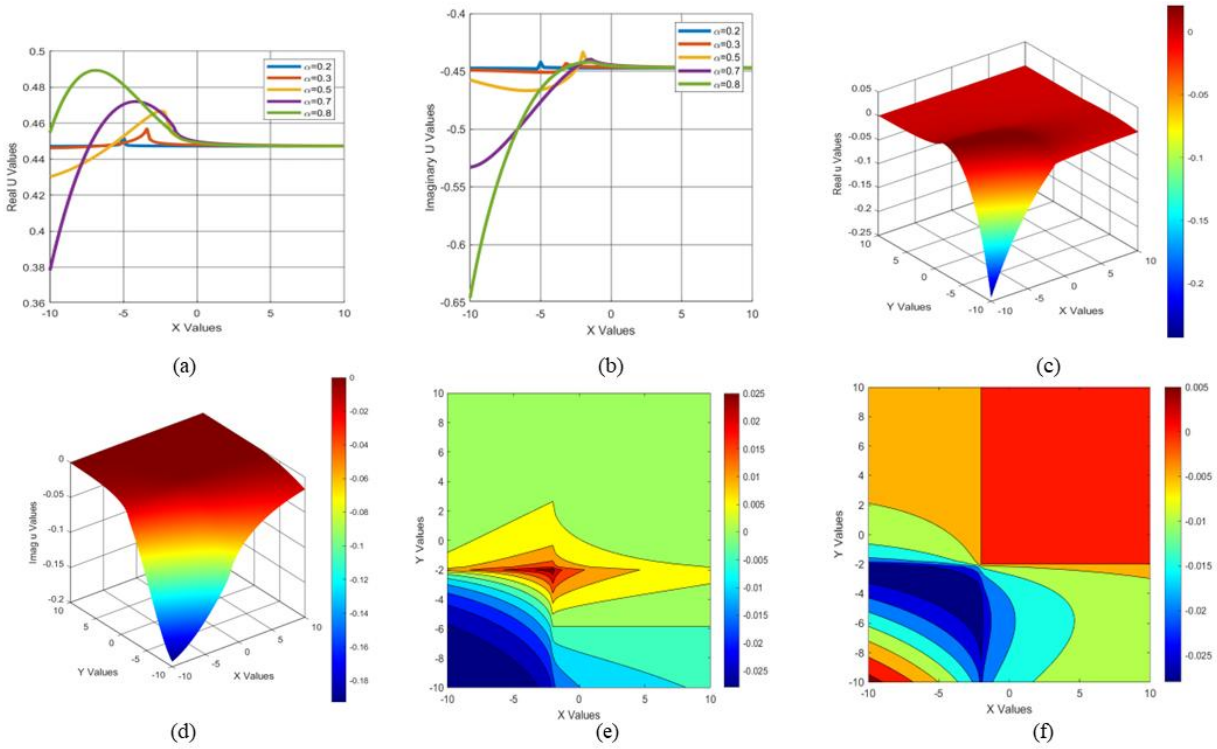

Figure 5. 2D, 3D, and contour profiles for the dark soliton solution of Eq (3.36) is obtained for certain values of $k = 0.1$, $l = 0.2$, $c = 0.3$, $w_0 = 0.5$, $w_1 = 0.0$, $w_2 = 0.5$, $r_1 = 0.2$, $\beta = 2$, $\alpha = 0.8$, and $t = 10$, thus showing its smooth transition and propagation over space and time.

5. Comparison

This study explores a comparative analysis of solutions derived from the modified S-expansion method, the modified simple equation method [12], and the $\exp(-\phi(\eta))$-expansion method [13], thereby focusing on their application to the SMCH equation. Each of these methods is a version of the modified simple equation method, and the $\exp(-\phi(\eta))$-expansion method serves as a distinct approach in mathematical physics, thereby offering unique features and advantages.

Islam et al. [13] applied the modified simple equation method to the SMCH equation, and obtained eight solutions under specific parameter conditions (See Appendix I). In contrast, our study utilized the modified S-expansion method, which yielded 31 distinct solutions characterized by hyperbolic, trigonometric, and exponential functions. These solutions significantly differ from those documented by Islam et al [13].

Meanwhile, Ali [12] explored the SMCH equation using the $\exp(-\phi(\eta))$-expansion method, and identified only five solutions (See Appendix II). However, by employing the modified S-expansion method, we derived a more extensive set of 31 solutions, once again expressed through hyperbolic, trigonometric, and exponential functions.

This comparative analysis underscores the diversity and scope of solutions each method can achieve, thus highlighting the modified S-expansion method's capacity to uncover a broader array of solutions for the SMCH equation.

6. Conclusions

This study unveiled a diverse and comprehensive collection of exact soliton solutions—including dark, bright, kink, anti-kink, and periodic solitons—that capture distinct features of solitary wave phenomena. The behavior and structure of these solutions were meticulously visualized through detailed 2D, 3D, and contour plots across both real and imaginary components, which revealed how various parameters influence their evolution and propagation. One of the hallmark strengths of the employed modified S-expansion method lies in its computational efficiency, which enables the swift derivation of exact solutions with significantly reduced complexity compared to traditional methods. In a comparative context, Islam et al. [13] employed the modified simple equation method to analyze the SMCH equation, and obtained eight specific solutions under constrained parameter conditions. Conversely, our study—through the modified S-expansion method—yielded a much broader set of 31 exact solutions involving hyperbolic, trigonometric, and exponential forms, and demonstrated a clear enhancement in solution diversity and scope. Likewise, Ali [12] applied the $\exp(-\phi(\eta))$-expansion method and derived only five solutions, whereas our approach consistently produced a more comprehensive family of 31 solutions under the same equation, further reinforcing the robustness and versatility of the modified S-expansion method. These outcomes accentuate the theoretical significance of the proposed approach and significantly improve its effectiveness in addressing real-world nonlinear phenomena. Looking ahead, this work opens promising avenues, including extending the methods to higher-dimensional systems, integrating machine learning and numerical simulations for an improved accuracy, and exploring the soliton stability and parameter sensitivity. Experimental validation in optical fibers, plasma, or fluid systems could further confirm the real-world relevance and impact of these findings.

Author contributions

Hamida Parvin: Conceptualization, Data curation, Formal analysis, Funding acquisition, Investigation, Methodology, Project administration, Resources, Software, Supervision, Validation, Visualization, Writing–original draft, Writing–review & editing. **Md. Nur Alam**: Project administration, Resources, Conceptualization, Writing–review & editing, Visualization, Methodology, Investigation, Validation, Formal analysis, Software, Supervision. **Md. Farhad Hossain:** Writing–review & editing, Writing–original draft, Supervision, Investigation, Conceptualization. **Mohammad Hassan:** Writing–review & editing, Writing–original draft, Supervision, Investigation, Conceptualization. **Md. Jakir Hossen**: Writing–Funding acquisition, review & editing, Supervision, Investigation, Conceptualization. All authors have read and approved the final version of the manuscript for publication.

Use of Generative-AI tools declaration

The authors declare that they have not used artificial intelligence (AI) tools in the creation of this article.

Conflict of interest

The authors declare that there is no conflict of interest.

References

1. O. G. Mustafa, A note on the Degasperis–Procesi equation, *J. Nonlinear Math. Phys.*, **12** (2005), 10–14. https://doi.org/10.2991/jnmp.2005.12.1.2
2. H. Lundmark, J. Szmigielski, Multi-peakon solutions of the Degasperis–Procesi equation, *Inverse Probl.*, **19** (2003), 1241–1265. https://doi.org/10.1088/0266-5611/19/6/001
3. A. M. Wazwaz, New solitary wave solutions to the modified forms of Degasperis–Procesi and Camassa–Holm equations, *Appl. Math. Comput.*, **186** (2007), 130–141. https://doi.org/10.1016/j.amc.2006.07.092
4. A. M. Wazwaz, Solitary wave solutions for modified forms of Degasperis–Procesi and Camassa–Holm equations, *Phys. Lett.* A, **352** (2006), 500–504. https://doi.org/10.1016/j.physleta.2005.12.036
5. R. Camassa, D. D. Holm, An integrable shallow water equation with peaked solitons, *Phys. Rev. Lett.*, **71** (1993), 1661–1664. https://doi.org/10.1103/PhysRevLett.71.1661
6. L. Tian, X. Song, New peaked solitary wave solutions of the generalized Camassa–Holm equation, *Chaos Soliton. Fract.*, **19** (2004), 621–637. https://doi.org/10.1016/S0960-0779(03)00192-9
7. J. P. Boyd, Peakons and coshoidal waves: Traveling wave solutions of the Camassa–Holm equation, *Appl. Math. Comput.*, **81** (1997), 173–187. https://doi.org/10.1016/0096-3003(95)00326-6
8. A. M. Wazwaz, New compact and noncompact solutions for two variants of a modified Camassa–Holm equation, *Appl. Math. Comput.*, **163** (2005), 1165–1179. https://doi.org/10.1016/j.amc.2004.06.005
9. A. Irshad, M. Usman, S. T. Mohyud-Din, Exp-function method for simplified modified Camassa-Holm equation, *Int. J. Modern Math. Sci.*, **4** (2012), 146–155.
10. N. H. Ali, S. A. Mohammed, J. Manafian, Study on the simplified MCH equation and the combined KdV–mKdV equations with solitary wave solutions, *Partial Differ. Equ. Appl. Math.*, **9** (2024), 100599. https://doi.org/10.1016/j.padiff.2023.100599
11. Z. R. Liu, R. Q. Wang, Z. J. Jing, Peaked wave solutions of Camassa–Holm equation, *Chaos Soliton. Fract.*, **19** (2004), 77–92. https://doi.org/10.1016/S0960-0779(03)00082-1
12. A. Ali, M. A. Iqbal, S. T. Mohyud-Din, Traveling wave solutions of generalized Zakharov–Kuznetsov–Benjamin–Bona–Mahony and simplified modified form of Camassa–Holm equation exp(–φ(η))–expansion method, *Egypt. J. Basic Appl. Sci.*, **3** (2016), 134–140. https://doi.org/10.1016/j.ejbas.2016.01.001
13. M. N. Islam, M. Asaduzzaman, M. Shajib Ali, Exact wave solutions to the simplified modified Camassa–Holm equation in mathematical physics, *AIMS Mathematics*, **5** (2019), 26–41. https://doi.org/10.3934/math.2020003
14. G. Zhang, M. Zhang, New explicit exact traveling wave solutions of Camassa–Holm equation, *Appl. Anal.*, **104** (2025), 69–81. https://doi.org/10.1080/00036811.2021.1986024

15. A. Aasaraai, The application of modified F-expansion method solving the Maccari's system, *J. Adv. Math. Comput. Sci.*, **11** (2015), 1–14. https://doi.org/10.9734/BJMCS/2015/19938
16. A. R. Alharbi, Traveling-wave and numerical solutions to nonlinear evolution equations via modern computational techniques, *AIMS Mathematics*, **9** (2024), 1323–1345. https://doi.org/10.3934/math.2024065

Appendix

Appendix I. The list of solutions to the SMCH equation that was examined using the approach (Islam et al. [13]) is presented in this part and is organized as follows:

$$\Theta_{(1,2)} = \pm\frac{i\sqrt{3(w-2k)}}{\sqrt{\beta}}\ \cot\left(\frac{\sqrt{(w-2k)}\xi}{\sqrt{2k}}\right). \tag{A1.1}$$

$$\Theta_{(3,4)} = \pm\frac{i\sqrt{3(w-2k)}}{\sqrt{\beta}}\ \tan\left(\frac{\sqrt{(w-2k)}\xi}{\sqrt{2k}}\right). \tag{A1.2}$$

$$\Theta_{(5,6)} = \pm\frac{i\sqrt{3(2k-w)}}{\sqrt{\beta}}\ \coth\left(\frac{\sqrt{(2k-w)}\xi}{\sqrt{2k}}\right). \tag{A1.3}$$

$$\Theta_{(7,8)} = \pm\frac{i\sqrt{3(2k-w)}}{\sqrt{\beta}}\ \tanh\left(\frac{\sqrt{(2k-w)}\xi}{\sqrt{2k}}\right). \tag{A1.4}$$

Appendix II. The list of solutions to the SMCH equation that was examined using the approach (Ali et al. [12]) is presented in this part and is organized as follows:

$$\Theta_1 = a_0 - \frac{2\mu\sqrt{6}}{-\sqrt{\lambda^2-4\mu}\tanh\left(\frac{\sqrt{\lambda^2-4\mu}}{2}(\xi+c_1)\right)-a_0)}. \tag{A2.1}$$

$$\Theta_2 = a_0 - \frac{2\mu\sqrt{6}}{\sqrt{-\lambda^2+4\mu}\tan\left(\frac{\sqrt{-\lambda^2+4\mu}}{2}(\xi+c_1)\right)-a_0)}. \tag{A2.2}$$

$$\Theta_3 = a_0 - \frac{\lambda\sqrt{6}}{exp((\xi+c_1)^{\lambda}-1)}. \tag{A2.3}$$

$$\Theta_4 = a_0 - \frac{\sqrt{6}(\xi+c_1)\lambda^2}{(2(\xi+c_1)^{\lambda}+2)}. \tag{A2.4}$$

$$\Theta_5 = a_0 - \frac{\sqrt{6}}{(\xi+c_1)}. \tag{A2.5}$$